AD-A141 565 SENSITIVITY OF A LIDAR INVERSION ALGORITHM TO PARAMETERS RELATING ATMOSPH..(U) NAVAL OCEAN SYSTEMS CENTER SAN DIEGO CA H G HUGHES ET AL. APR 84 1/1

UNCLASSIFIED NOSC/TD-695 F/G 4/1 NL

END
DATE FILMED
7 84
DTIC

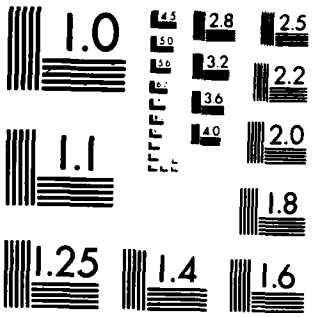

MICROCOPY RESOLUTION TEST CHART
NATIONAL BUREAU OF STANDARDS-1963-A

(12)

NOSC TD 695

NOSC TD 695

Technical Document 695

SENSITIVITY OF A LIDAR INVERSION ALGORITHM TO PARAMETERS RELATING ATMOSPHERIC BACKSCATTER AND EXTINCTION

H. G. Hughes
D. H. Stephens
J. A. Ferguson

April 1984
Final Report

Prepared for
Naval Air Systems Command
(NAVAIR 330)

Approved for public release; distribution unlimited

NOSC

NAVAL OCEAN SYSTEMS CENTER
San Diego, California 92152

NAVAL OCEAN SYSTEMS CENTER SAN DIEGO, CA 92152

AN ACTIVITY OF THE NAVAL MATERIAL COMMAND

J.M. PATTON, CAPT, USN
Commander

R.M. HILLYER
Technical Director

ADMINISTRATIVE INFORMATION

This task was performed for the Naval Air Systems Command (NAVAIR 330), under program element 62759N, subproject WF59551. The work was carried out by the Naval Ocean Systems Center (Code 5325), San Diego, CA 92152.

Released by
J. H. Richter, Head
Ocean and Atmospheric
Sciences Division

Under authority of
J. D. Hightower, Head
Environmental Sciences
Department

PK

UNCLASSIFIED

SECURITY CLASSIFICATION OF THIS PAGE (When Data Entered)

REPORT DOCUMENTATION PAGE		READ INSTRUCTIONS BEFORE COMPLETING FORM
1. REPORT NUMBER NOSC TD 695	2. GOVT ACCESSION NO. AD-A141565	3. RECIPIENT'S CATALOG NUMBER
4. TITLE (and Subtitle) SENSITIVITY OF A LIDAR INVERSION ALGORITHM TO PARAMETERS RELATING ATMOSPHERIC BACKSCATTER AND EXTINCTION		5. TYPE OF REPORT & PERIOD COVERED Final 6. PERFORMING ORG. REPORT NUMBER
7. AUTHOR(s) H.G. Hughes D.H. Stephens J.A. Ferguson		8. CONTRACT OR GRANT NUMBER(s)
9. PERFORMING ORGANIZATION NAME AND ADDRESS Naval Ocean Systems Center (Code 5325) San Diego, CA 92152		10. PROGRAM ELEMENT, PROJECT, TASK AREA & WORK UNIT NUMBERS 62759N WF59551
11. CONTROLLING OFFICE NAME AND ADDRESS Naval Air Systems Command (NAVAIR 330) Washington, DC 20361		12. REPORT DATE April 1984 13. NUMBER OF PAGES 16
14. MONITORING AGENCY NAME & ADDRESS(if different from Controlling Office)		15. SECURITY CLASS. (of this report) Unclassified 15a. DECLASSIFICATION/DOWNGRADING SCHEDULE

16. DISTRIBUTION STATEMENT (of this Report)

Approved for public release; distribution unlimited

17. DISTRIBUTION STATEMENT (of the abstract entered in Block 20, if different from Report)

18. SUPPLEMENTARY NOTES

19. KEY WORDS (Continue on reverse side if necessary and identify by block number)

Lidar
Single-scattering
Extinction
Visioceilometer

20. ABSTRACT (Continue on reverse side if necessary and identify by block number)

A lidar return from a homogeneous atmosphere is used to examine the sensitivity of an inversion algorithm to uncertainties in parameters in a power law relating backscatter to extinction.

DD FORM 1 JAN 73 1473 EDITION OF 1 NOV 65 IS OBSOLETE
S/N 0102-LF-014-6601

UNCLASSIFIED

SECURITY CLASSIFICATION OF THIS PAGE (When Data Entered)

INTRODUCTION

In an earlier paper, Klett[1] presented a stable solution to the single-scattering lidar equation

$$S(r) \equiv \ln[P(r)r^2] = \ln[C_1C_2] + k \ln\sigma(r) - 2\int_o^r \sigma(r)dr. \quad (1)$$

In this equation P(r) is the power received at a range r and C_1 is $P_o\frac{c\tau AF}{2}$ where P_o is the transmitted power, c is the speed of light, τ is the pulse width, A is the receiver area and F is the overall system response. The constants C_2 and k are atmospheric dependent parameters which relate the coefficients of backscatter, $\beta_\pi(r)$, and extinction, $\sigma(r)$, according to the power law relationship[1]

$$\beta_\pi(r) = C_2\sigma(r)^k. \quad (2)$$

From Equation (1) a differential equation (independent of C_1 and C_2)

$$\frac{dS(r)}{dr} = \frac{k}{\sigma(r)}\frac{d\sigma(r)}{dr} - 2\sigma(r) \quad (3)$$

can be obtained which has the well known solution

$$\sigma(r) = \frac{\exp\{[S(r) - S(r_o)]/k\}}{\sigma(r_o)^{-1} - \frac{2}{k}\int_{r_o}^{r}\exp\{[S(r) - S(r_o)]/k\}dr}, \quad (4)$$

where $\sigma(r_o)$ is the extinction coefficient at a range r_o. This range is normally chosen where the transmitted beam and receiver field-of-view overlap. In this equation the extinction is detemined by the ratio of two

numbers which each become smaller as r increases. In particular, for good visibilities the denominator becomes the difference between large numbers and small flucuations in S(r) can cause large oscillations in $\sigma(r)$. Klett[1] also discusses the instabilities in $\sigma(r)$ caused by uncertainties in estimating $\sigma(r_o)$. He proposed a more stable solution to Equation (3) for $r<r_f$ rather than $r>r_o$. This new solution is

$$\sigma(r) = \frac{\exp\{[S(r) - S(r_f)]/k\}}{\sigma(r_f)^{-1} + \frac{2}{k}\int_r^{r_f}\exp\{[S(r) - S(r_f)]/k\}dr} \qquad (5)$$

where $\sigma(r_f)$ is the extinction coefficient at range r_f. In this case it is not possible for the denominator to become zero or negative and $\sigma(r)$ is determined by the ratio of two numbers which become larger as r decreases from r_f.

Recently, Ferguson and Stephens[2] described a novel approach in determining $\sigma(r)$ using both Equations (4) and (5). In their algorithm an iterative scheme is used to select the appropriate value of $\sigma(r)$ using Equation (5). A value of $\sigma(r)$ is determined such that the value of $S_c(r)$ calculated from Equation (1) matches the measured value $S_m(r)$. The iteration procedure is initiated at a close-in range where the returned signal is well above the system noise and requires a minimum amount of computational time. To demonstrate the utility of their algorithm, Ferguson and Stephens[2] presented examples of calculated and measured values of S(r) normalized to the product C_1C_2. RMS differences of less than 10^{-4} over the range r_o to r_f indicate the value of $\sigma(r_f)$ to be very accurate. This value was then used as $\sigma(r_o)$ in Equation (4) to determine $\sigma(r)$ for $r>r_f$. In this case it is possible to extend $\sigma(r)$ out to ranges where $S_m(r)$ disappears into system noise. However,

it must be realized that the solution for $\sigma(r)$ is not unique unless the values of C_2 and k along the propagation path are known. The proper choice of these parameters is a critical problem in interpretation of lidar returns. In his original paper, Klett[1] showed Equation (5) to be rather insensitive to changes in k for highly turbid atmospheres. Little attention has been given to the sensitivity of the inversion algorithms to changes in C_2 which is usually assumed to be invariant. However, from the work of Barteneva[3], a change greater than an order of magnitude can be inferred in the value of C_2 between clear air and fog conditions. Fitzgerald[4] has also pointed out that a power-law relationship between backscatter and extinction is only valid for relative humidities greater than about 80 percent and, even then, it is dependent upon the air mass characteristics.

In this paper, we investigate the sensitivity of the inversion algorithm to uncertainties in C_2 and k. For this study we utilized data acquired in September 1982 at a research site located near the Baltic Sea. The data were obtained using a handheld battery operated lidar, termed a "visioceilometer," developed by the U.S. Army for measuring atmospheric visibility and cloud heights.[5] The optical unit is a modified AN/GVS-5 laser rangefinder which emits a 10-m J, 6-nsec pulse at 1.06μm. The signal processing unit clocks the return signal through a transient recorder at a 20-MHz rate giving a 7.5 m sampling interval. The digitized results are transferred to a microprocessor and then to a tape recorder for off-line processing by a Hewlett-Packard 9845B computer.

INVERSION EXAMPLES AND ANALYSIS

For this study we have chosen a lidar return obtained during reduced visibility conditions for which the Klett inversion (Equation 5) rapidly

converges. Figure 1 is a plot of S(r) versus range determined from a lidar return. The initial slope of the curve shows a nearly monotonic decrease with range and indicates a homogeneous atmosphere out to nearly 500 m. In this case, (from Equation 1) the extinction coefficient is given by $-\frac{1}{2}\frac{dS(r)}{dr}$. Beyond 500 m the atmosphere appears less homogeneous and may represent a variation with altitude as the lidar was elevated 3°. Here we will limit the analysis to the homogeneous portion of the return between ranges r_o = 112.5 m and r_f = 412.5 m. For this portion of the curve, a least squares straight line fit (with a correlation coefficient of 0.956) gives

$$S(r) = -1.68r - 4.98 \tag{6}$$

from which the homogeneous extinction coefficient σ_o is determined to be 0.84 km^{-1}. By equating Equation (6) to Equation (1) for the homogeneous case we find (for k = 1)

$$\ln[C_1 C_2] = -4.8. \tag{7}$$

If the system constant C_1 is known, then C_2 is determined for this special case. However, since the overall system response of the visioceilometer is not known, we will in fact determine the sensitivity of the algorithm to uncertainties in the parameter $\ln[C_1 C_2']$ which are directly related to variations in C_2 (for fixed values of k) by the expression

$$\ln[C_1 C_2'] = \ln[C_2'/C_2] - 4.8 \tag{8}$$

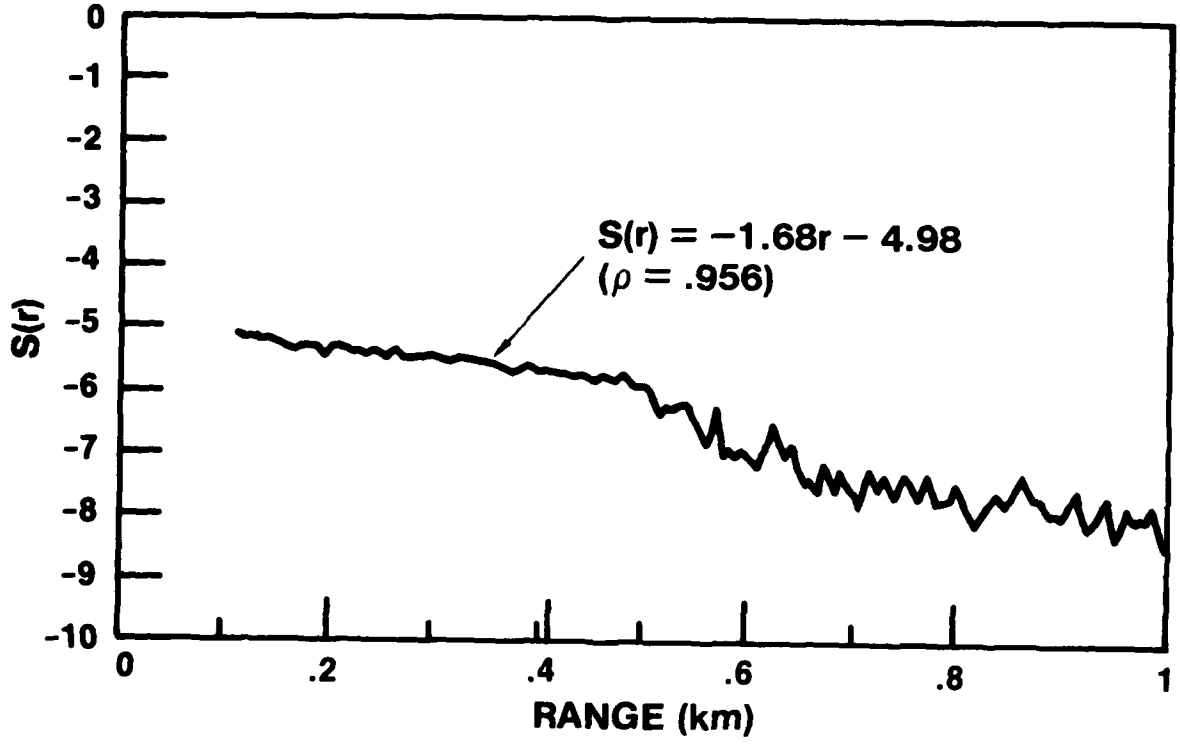

Figure 1. S(r) versus range determined from a lidar return.

Accession For	
NTIS GRA&I	☑
DTIC TAB	☐
Unannounced	☐
Justification	
By	
Distribution/	
Availability Codes	
Dist	Avail and/or Special
A-1	

where C_2' differs from the correct value, C_2. In Figure 2 the value of C_2' is allowed to change by ±40% from C_2 with resulting changes in $\ln[C_1C_2']$ from +7% to -10%.

Figures 3A to I are plots of the extinction coefficients calculated using the values of $\ln[C_1C_2']$ shown in each figure and the S(r) values from Figure 1 with k = 1. For these calculations the RMS differences between the measured and calculated values of S(r) ranged between 10^{-2} and 10^{-4}. The extinction coefficient in Figure 3E $\left(\ln[C_1C_2'] = -4.79\right)$ is nearly constant out to 500 m and is in close agreement with that determined from the slope of S(r) in Figure 1. However, for the cases where $C_2'/C_2 < 1$ (Figures 3A to D), the calculated extinctions increase with range to a value near 4 km^{-1} in Figure 3A. When $C_2'/C_2 > 1$ (Figures 3F to I) the extinction coefficients decrease with range and tend towards zero in Figure 3I. These tendencies are similiar to the singularities and zeros discussed by Klett[1] when the inversion is started at the beginning of the return signal.

Also listed in the figures are the visibilities determined from the relation

$$VIS = \frac{3.912\ (r_f - r_o)}{\int_{r_o}^{r_f} \sigma(r)dr} . \qquad (9)$$

In Figure 4 the calculated visibilities are plotted for the relative changes in C_2 and differing values of k. In general, these calculations show the visibility to be rather insensitive to k. However, we have found the extinction coefficients to be sensitive to small changes in k when σ(r) is at or approaching a singularity as in Figures 3A and 3B. The sensitivity of

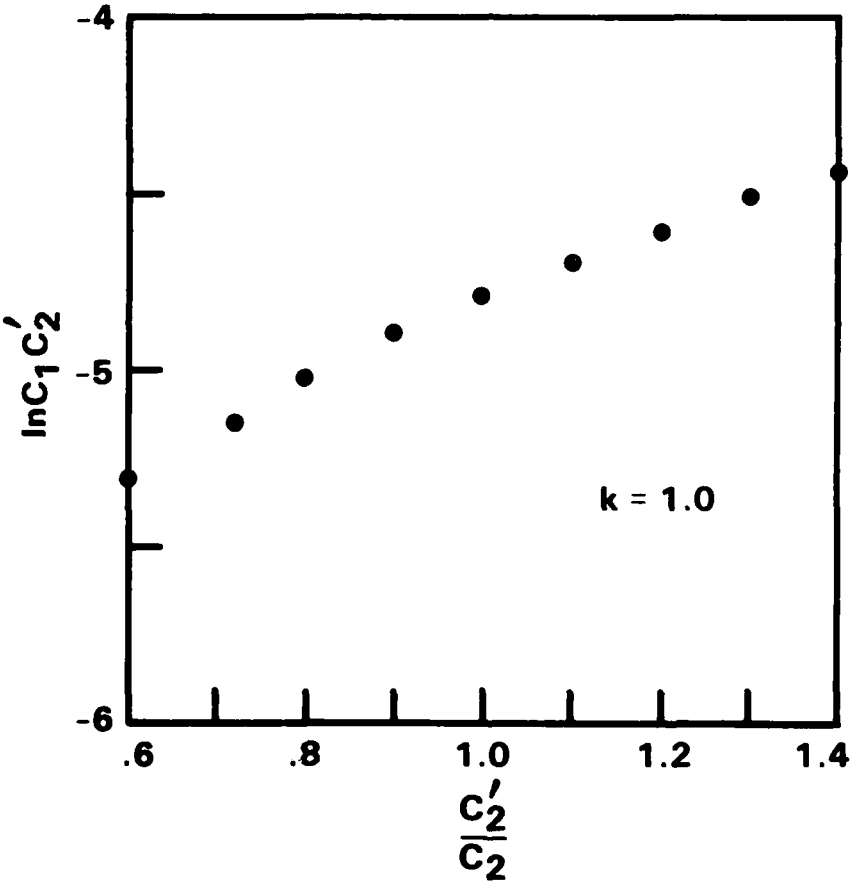

Figure 2. Changes in the parameter $\ln[C_1 C_2']$ with changes in the value of C_2 appropriate for Equation 7.

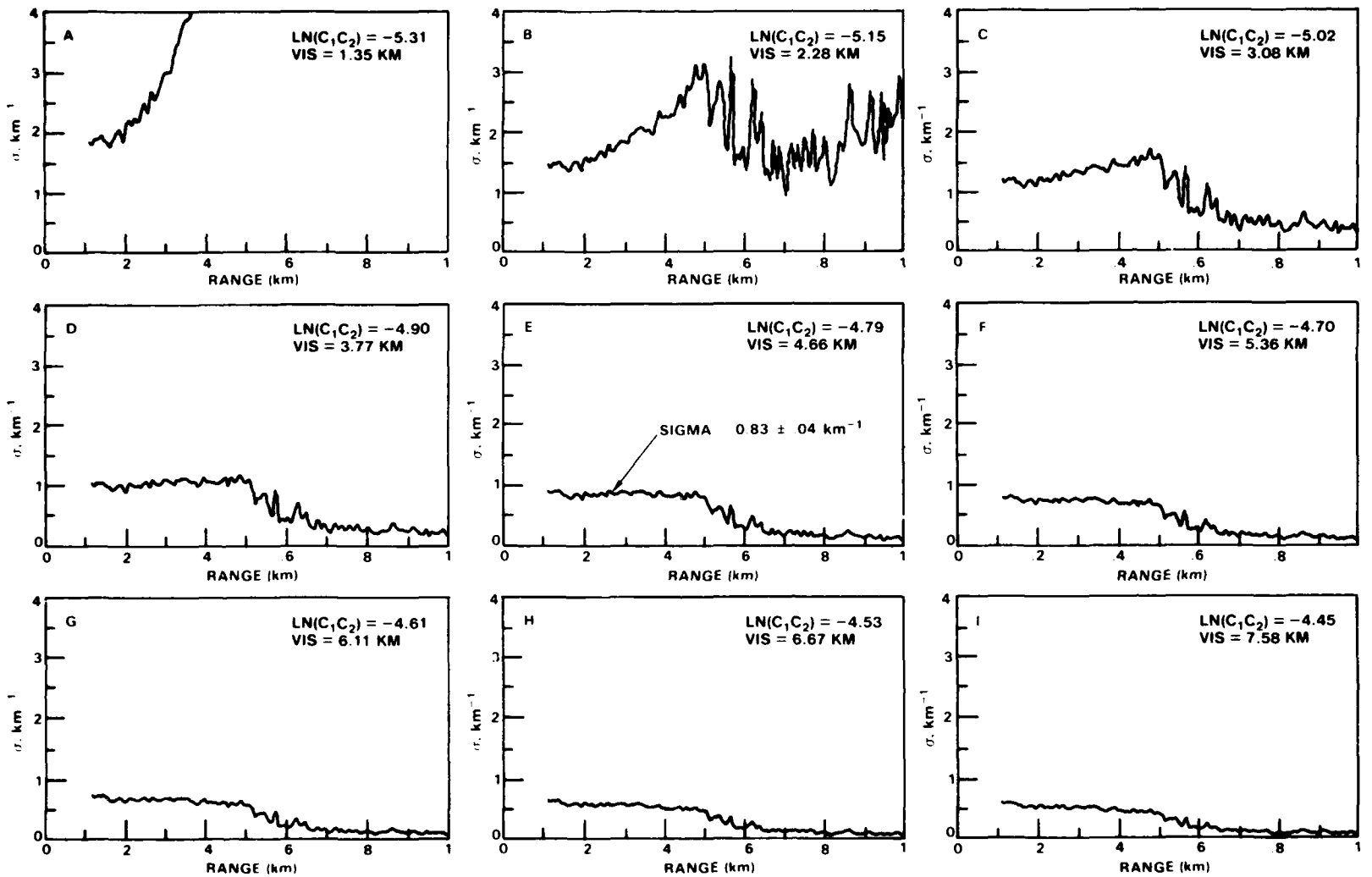

Figure 3. Calculated values of extinction coefficient $\sigma(r)$ as a function of range for different values of the parameter $\ln[C_1C_2']$.

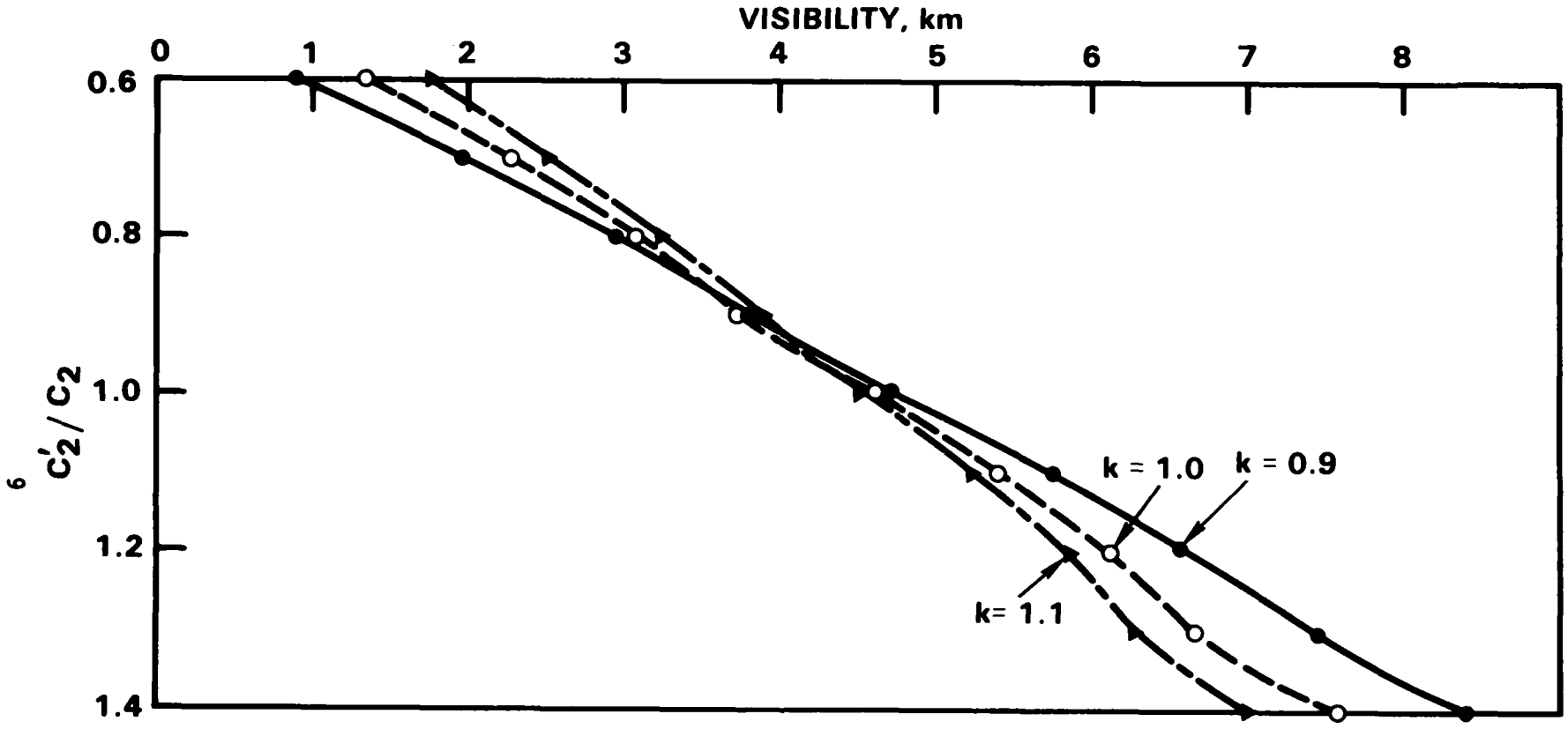

Figure 4. Calculated visibilities for relative changes in C_2 for differing values of k.

visibility to relative uncertainties in C_2 is seen in Figure 4 where a 20 percent uncertainty can cause nearly a 30 percent change in visibility.

The variations of extinction coefficients with range can be explained for a uniform atmosphere $[\sigma(r) = \sigma_o]$ if we use values of C_2' and $\sigma'(r)$ to evaluate the closeness of the measured and calculated values of S(r), i.e.,

$$S_m(r) \equiv S_c(r) \tag{10}$$

or

$$\ln[C_1C_2] + k\ln(\sigma_o) - 2\sigma_o r = \ln[C_1C_2'] + k\ln\sigma'(r) - 2\sigma'(r_o)\, r_o - 2\int_{r_o}^{r} \sigma'(r)dr. \tag{11}$$

Rearranging gives

$$-\ln[C_2'/C_2] + k\ln[\sigma_o/\sigma'(r)] - 2\sigma_o r + 2\sigma'(r_o)\, r_o + 2\int_{r_o}^{r} \sigma'(r)dr = 0\ . \tag{12}$$

For a uniform atmosphere,

$$S_m(r) - S_m(r_o) = -2\sigma_o(r - r_o) \tag{13}$$

and $\sigma'(r)$ are then determined from Equation (4) to be (for k = 1)

$$\sigma'(r) = \frac{\exp[-2\sigma_o(r - r_o)]}{\sigma'(r_o)^{-1} - 2\int_{r_o}^{r} \exp[-2\sigma_o(r - r_o)]dr} \tag{14}$$

from which $\sigma'(r_o)$ is determined to be

$$\sigma'(r_o) = \frac{\sigma_o}{[\sigma_o/\sigma'(r) - 1]\exp[-2\sigma_o(r - r_o)] + 1} . \tag{15}$$

The integral term in Equation (12) is also readily determined from tables to be

$$2\int_{r_o}^{r} \sigma'(r)dr = -\ln\left\{\frac{(\sigma_o/\sigma'(r))\exp[-2\sigma_o(r - r_o)]}{[(\sigma_o/\sigma'(r)) - 1]\exp[-2\sigma_o(r - r_o)] + 1}\right\} , \tag{16}$$

and upon substitution of Equations (15) and (16) into (12) we arrive at the equation

$$\ln\chi = 2\,\sigma_o r_o\left(1 - \frac{1}{\chi}\right) + \ln[C_2'/C_2] \tag{17}$$

where

$$\chi = [\sigma_o/\sigma'(r) - 1]\exp[-2\sigma_o(r - r_o)] + 1 \tag{18}$$

and

$$\sigma'(r) = \frac{\sigma_o}{1 + (\chi - 1)\exp[2\sigma_o(r - r_o)]} . \tag{19}$$

It is then seen that for $\chi < 1$, $\sigma'(r)$ becomes infinite at a range

$$r - r_o = -\frac{1}{2\sigma_o}\ln(1 - \chi) . \tag{20}$$

For $\chi > 1$ we find that $\sigma'(r) \to 0$ as $r \to \infty$. Denoting the left and right sides of Equation (17) as $f_1(\chi)$ and $f_2(\chi)$, respectively, a graphical solution to the equation is presented in Figure 5 for $\sigma_o = 0.85\ km^{-1}$. From the curves it is seen that $\chi > 1$ when $C_2'/C_2 > 1$ and $\chi < 1$ for $C_2'/C_2 < 1$. An example of a numerical solution of Equation (17) is shown in Figure 6 which illustrates the behavior of $\sigma'(r)$ with range for uncertainties in C_2. If C_2 is underestimated, $\sigma'(r)$ tends to increase without bound. If C_2 is underestimated by 20 percent, $\sigma'(r)$ differs from the known σ_o by a factor of 4 at a range less than 1 km. If C_2 is over estimated, $\sigma'(r)$ tends to zero. These trends in $\sigma'(r)$ are identical to those illustrated from the measured data in Figure 3.

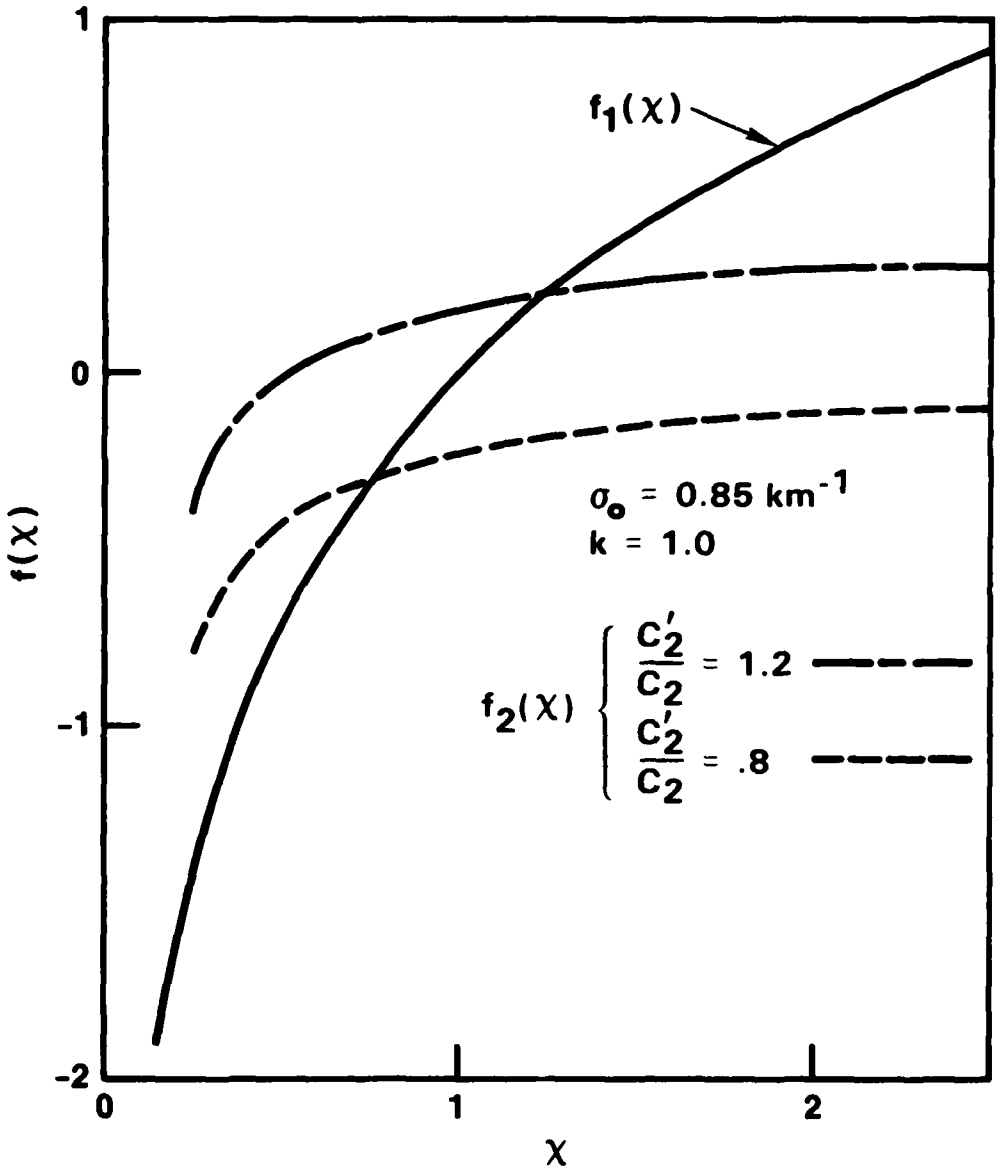

Figure 5. Graphical solution of the parameter χ in Equation (17) for relative changes in C_2.

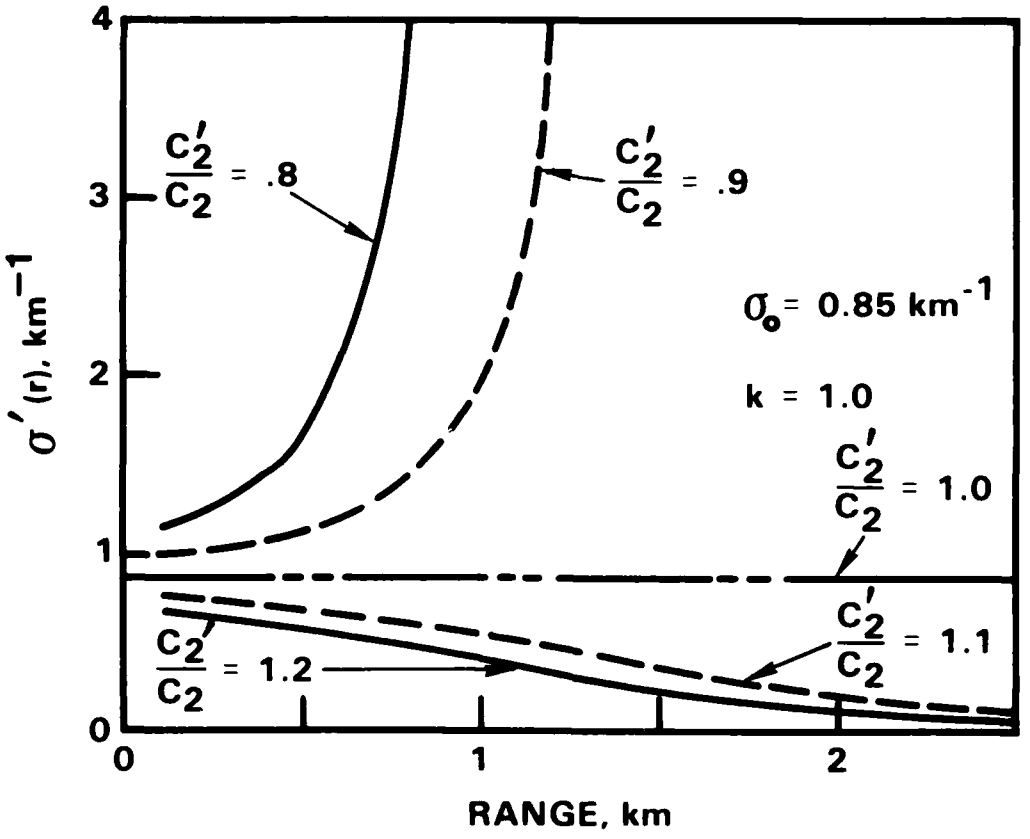

Figure 6. Numerical solution of Equation (17) for $\sigma'(r)$ versus range for relative changes in C_2.

CONCLUSIONS

This analysis has determined that range dependent extinction coefficients inferred from lidar returns are extremely sensitive to the value of the constant relating backscatter and extinction for a reduced visibility condition. The instabilities will also occur for better visibilities but at longer ranges. A correct interpretation of atmospheric structure deduced from lidar data requires precise knowledge of C_2 along the path. It is also important to realize that changes in extinction coefficients occur with changes in the product C_1C_2. Uncertainties or instabilities in the system constant C_1 can result in similar instabilities in the extinction coefficient.

REFERENCES

1. Klett, JD, Stable Analytical Inversion Solution for Processing Lidar Returns, Applied Optics, Vol 20, p 211, 1981.

2. Ferguson, JA and Stephens, DH, Algorithm for Inverting Lidar Returns, Applied Optics, Vol 22, p 3673, 1983.

3. Barteneva, OD, Scattering Functions of Light in the Atmospheric Boundary Layer, Bulletin of the Academy of Sciences, USSR, Geophysics Series, p 12, 32-1244, 1960.

4. Fitzgerald, JA, The Effect of Relative Humidity on the Aerosol Back-scattering Coefficient at 0.694 and 10.6μm Wavelengths, Applied Optics, Vol 23, p 411, 1984.

5. ASL TR 0105, The Visioceilometer: A Portable Visibility and Cloud Ceiling Height Lidar, by W.J. Lentz, 1982.